African Journal of Pure and Applied Chemistry Vol. 6(13), pp. 204-213, November 2012
Available online at http://www.academicjournals.org/AJPAC
DOI: 10.5897/AJPAC12.011
ISSN 1996 - 0840 ©2012 Academic Journals

Full Length Research Paper

Complexes of Nile Red and β- or γ-cyclodextrin: A semiempirical-density functional theory-molecular dynamics route

Ruth Hojvat[1,2], Dora A. Barbiric[3] and Eduardo A. Castro[4]*

[1]Facultad de Ciencias Exactas y Naturales, Universidad de Belgrano, Zabala 1837 CABA (CP 1426DQG) Argentina.
[2]Escuela de Tecnología y Escuela de Ciencias Agrarias, Universidad Nacional del Noroeste de la Provincia de Buenos Aires, Sede Junin, R. Sáenz Peña 456, Junín B6000, Pcia de Buenos Aires, Argentina.
[3]Facultad de Ingeniería, Universidad de Buenos Aires, Av. Paseo Colón 850, C1063ACV, Buenos Aires, Argentina.
[4]Instituto de Investigaciones Fisicoquímicas Teóricas y Aplicadas, Universidad Nacional de La Plata, Suc. 4, C.C. 16, 1900La Plata, Buenos Aires, Argentina.

Accepted 5 October, 2012

The association of Nile Red (NR) with β-, and γ-cyclodextrins (CDs) was analyzed by semiempirical parametric method 3 (PM3), density functional theory-Becke, three-parameter, Lee-Yang-Parr hybrid functional (DFT-B3LYP/6-31G), and molecular dynamics (MD) and Langevin dynamics (LD) calculations, including annealing and molecular mechanics (MM) geometry optimization. Our results suggest that inclusion complexes of NR and both CD are possible but occlusion complexes are more favourable. Differences in the intermolecular H-bonding yielded by the DFT-level of treatment could explain the distinct behaviour regarding deactivation to the ground state of NR in presence of β-, and γ-CD in fluorescence experiments. DFT optimization of NR in gaseous state rendered lower twisting angles and larger pyramidalization of the amino group than reported elsewhere.

Key words: Molecular modeling, cyclodextrins, Nile Red complexes.

INTRODUCTION

Nile Red (NR), that is, *9*-diethylamino-5*H*-benzo[α]-phenoxazine-5-one, is a laser dye, highly sensitive to the polarity of the environment. In 1985, it was shown that NR will fluoresce in a nonpolar environment and could serve as a probe to detect nonpolar lipids in cells (Greenspan and Fowler, 1985). NR permeates all structures within a cell, but the characteristic yellow fluorescence (approximately 575 nm) only occurs when the dye is in a nonpolar environment, primarily neutral storage lipid droplets. Thanks to the photochemical stability and strong fluorescence nature of NR, it has been used as probe in many different applications in materials science and in biology, when the polarity of the medium needs to be explored (Deye et al., 1990). NR has thus been applied to determine the polarity of conventional solvents and binary mixtures (Dutta et al., 1996; Uusi-Penttilä et al., 1997; Kipkemboi and Easteal, 1994) and of supercritical fluids (Berger and Deye, 1990), and used to probe the microenvironment of polymers (Dutta et al., 1996), xerogels (Matsui and Nozawa, 1997), liquid crystals (Choi et al., 1997), zeolites (Meinershagen and Bein, 1999; Uppili et al., 2000), micelles (Datta et al., 1997; Maiti et al., 1997) and lipid bilayers (Freeman et al., 2001). It has also been incorporated, as the sensing element, in fiber-optic devices capable of identifying and quantifying a range of organic vapors (White et al., 1996; Johnson et al., 1997).

*Corresponding author. E-mail: eacast@gmail.com.

Abbreviations: B3LYP, Becke, three-parameter, Lee-Yang-Parr hybrid functional; **CAM-B3LYP,** Coulomb-attenuating method-B3LYP; **CD,** cyclodextrin; **DFT,** density functional theory; **H-bond,** hydrogen bond; **HOMO,** highest occupied molecular orbital; **LD,** Langevin dynamics; **LUMO,** lowest unoccupied molecular orbital; **MD,** molecular dynamics; **MM,** molecular mechanics; **NR,** Nile Red; **PICT,** planar intramolecular charge transfer; **PM3,** semiempirical parametric method 3; **TICT,** twisted intramolecular charge transfer.

On the other hand, cyclodextrins (CDs) are cyclic oligosaccharide produced by degradation of the amylose fraction of starch by glucosyltransferases, as one or several turns of the amylose helix are hydrolyzed off and their ends are joined together. A family of macrocycles with different numbers of glucose units are thus produced (Szejtli, 1988; Duchêne, 1987), but the most abundant are α-, β-, and γ-CD with six, seven and eight glucopyranose units, respectively. These doughnut shaped molecules have been investigated with the use of spectroscopic, kinetic and crystallographic methods (Szejtli, 1988; Duchêne, 1987; Saenger, 1980, 1984; Harata, 1991; Saenger et al., 1998). They are frequently characterized as truncated cones, with the secondary hydroxyl groups of the glucopyranose units situated on the wide edge of the cone, and the primary hydroxyls placed on the narrow edge or rim. The cavity is lined by the hydrogen atoms and the glycosidic oxygen bridges (Szejtli, 1998). In an aqueous solution, the slightly apolar CD cavity is occupied by high enthalpy water molecules. These water molecules can be readily substituted by less polar guest molecules. Most frequently the host:guest ratio is 1:1, but other stoichiometries are also possible.

NR is insoluble in water but freely soluble in organic solvents and it forms association complexes with β- and γ-CD which are soluble in water. According to experimental results (Srivatsavoy, 1999), the presence of multiple inclusion complexes of NR with β- and γ-CD was inferred, but with clear differences between the two CDs. For example, a much longer fluorescence lifetime in β-CD complexes (1.2 ns for the major component) as compared to γ-CD complexes (40 ps for the major component) was observed. This difference was ascribed to the effect of inclusion on the twisted intramolecular charge transfer (TICT) decay process in NR: its effect is negligible as regards β-CD, but substantial when involving γ-CD (Datta et al., 1997). The non-radiative deactivation of NR from its singlet excited state involves the electron donor diethylamino group and the electron acceptor carbonyl group attached to the same aromatic ring; in polar solvents, the flexible dialkylamino group could undergo twisting, which makes the donor orbital perpendicular to the acceptor orbital. The NR fluorescence lifetime reduction could be explained, if inclusion into γ-CD would somehow result in a considerable enhancement of the TICT decay process in NR.

However, there is literature laying stress on the possibility that in the case of NR, the TICT process does not occur. Cser et al. (2002), based on the fluorescent properties of NR in different aprotic and protic solvents, concluded that the fluorescence lifetime of NR is not sensitive to dielectric solvent–solute interactions but markedly decreases with the increase of the hydrogen bond (H-bond) donating ability in alcohols because vibrations associated with H-bonding are involved in the radiationless deactivation to the ground state process. Moreover, the negligible viscosity effect that they observed would indicate that twisting of the diethylamino moiety of NR does not play a significant role in the dissipation of the excitation energy. This appears coherent with the results reported by Dias et al. (1999, 2006), whose theoretical studies of NR by *ab initio* and semiempirical methods showed that NR is planar in the ground state with a high barrier to rotation of the diethylamino group by 90° and the charge transfer decreases after the twisting in contrast to the TICT predictions. Kawski et al. (2009) reached the same conclusion, after having analyzed the solvatochromic (Kawski et al., 2008) and thermochromic (Kawski et al., 2009) effects on absorption and fluorescence spectra of NR in several solvents; the difference between the dipole moments corresponding to the ground and excited states of NR is too small for a TICT state that should show nearly full charge transfer. Recent results (Guido et al., 2010) obtained by applying a time-dependent density functional theory (DFT) approach and taking into account bulk solvent effects appear to support this interpretation. The authors investigated the absorption and fluorescence spectra of NR by assessing both the planar intramolecular charge transfer (PICT) and TICT mechanisms. They used a panel of exchange correlation function including both global and range-separated hybrids, refined solvent models and the simulation of vibronic couplings. Accurate Coulomb-attenuating method-Becke, three-parameter, Lee-Yang-Parr hybrid functional (CAM-B3LYP) (Yanai et al., 2004) results indicated that the two peaks observed in fluorescence spectra of NR in apolar solvents, often interpreted as dual fluorescence, are in fact the result of a strongly active vibronic coupling. This supports the PICT, rather than the TICT process.

The geometry and mode of inclusion of NR guest into the β- and γ-CD hosts was studied by Wagner et al. (2003), who used ultraviolet-visible (UV-Vis) absorption, steady state fluorescence and electrospray mass ionization spectroscopies, as well as molecular modeling. They suggested an association complex involving capping of the larger rim of the γ-CD cavity by NR, as opposed to an inclusion complex with the NR guest within the β-CD cavity. The same was proposed by Hazra et al. (2004), who reported about the effect of both β- and γ-CDs on the TICT in NR, after having performed steady state and time resolved fluorescence spectroscopy studies. They observed a much higher retardation of non-radiative rate for TICT of NR in the presence of β- than γ-CD. The little retardation in presence of γ-CD was attributed to the formation of H-bonds between the -OH groups of γ-CD with NR molecules, also verified by the large increase in rotational relaxation time and quantum yield of NR in γ-CD system on addition of urea. The formation of 1:1 or 1:2 capped complexes between NR and γ-CD was finally proposed.

Given the different results and especially interpretations

as to the possible structures of NR:CD complexes, the purpose of this work was to inquire, from the theoretical standpoint, about the association of NR with β- and γ-CD, as well as the stabilization and features of the resulting structures. Our analysis comprehends from molecular mechanics (MM) to molecular dynamics (MD), passing through semiempirical calculations and DFT. We intend to offer some rationalization for the spectroscopic behaviour that different authors reported and the structures of complexes that we have obtained.

METHOD

We have modeled *in vacuo* inclusion and occlusion complexes (1:1 stoichiometry only) by firstly submitting the system to MM+ method and then to a semiempirical parametric method 3 (PM3) optimization, both contained in the Hyperchem Pro 6.0 package for Windows. PM3 program was chosen because it was asserted to model H-bonding at best (Li et al., 2000; Zheng and Merz, 1992; Morley et al., 1997; Morpurgo et al., 1998) and was later even improved (McNamara and Hillier, 2007; Korth, 2010). To perform our calculations, we used structures of β-CD, γ-CD and NR earlier optimized by PM3 method. The guest NR was located either facing the primary or the secondary rim of the CD. From the set of association structures that were generated, selected complexes (the three NR:β-CD complexes with lowest, similar energies; same criterion for NR:γ-CD complexes) were later submitted to DFT calculations. Some NR:γ-CD inclusion complexes were submitted to dynamics simulations as well, in order to assess their viability. A more detailed description of the procedures are discussed.

Inclusion complexes

Simulations of the association processes were initiated by locating the guest, NR, with its longitudinal molecular axis perpendicular to the cyclic rim of the CD, at ~2.5 Å from the center of the rim. Additionally, NR systematically presented either the amino group or the opposite extreme ring oriented towards the cyclic rim of the CD. Due to the C1 symmetry of the PM3-optimized structures of both CDs, several starting orientations of NR were tried by rotating the latter about its longitudinal axis. Each time the system was relaxed and it evolved via MM treatment, towards a complex structure, each resulting complex underwent a PM3 optimization.

Previous reports referred to the possibility that multiple types of complexes may form with both types of CDs (Srivatsavoy, 1999). We therefore chose a set of the most stable complexes among those yielded by the procedure just described. These complexes were structurally distinct but with very similar PM3 energies ($\Delta E<0.04\%$, in kcal/mol). They were three NR:β-CD complexes and three NR:γ-CD complexes. We finally applied the DFT-B3LYP/6-31G calculation to them as implemented in the Gaussian 03 program (2003).

Occlusion complexes

We followed a similar procedure involving first MM+ and then PM3 calculations, but this time we started by locating the guest with its molecular plane parallel either to the primary or the secondary circular rim of the β-CD and γ-CD, and over the cavity opening. According to bibliography (Wagner et al., 2003; Hazra et al., 2004), after spectroscopic studies, it was suggested that occlusion complexes (that is, NR capping the CD cavity opening) are more likely in the case of γ-CD. Therefore, we submitted the four more stable occlusion structures involving β-CD and same number of complexes involving γ-CD that we obtained in this stage, to subsequent DFT-B3LYP/6-31G calculations. In the case of β-CD, two out of four complexes had the guest occluding the secondary rim. In the case of γ-CD, one out of four showed NR occluding the secondary rim.

Dynamics

It was suggested (Wagner et al., 2003) that γ-CD and NR would probably form unstable inclusion complexes. Given that we did obtain NR:γ-CD inclusion structures, we chose to test further the stability of the three NR:γ-CD complexes previously mentioned. We submitted them to dynamics simulations combined with MM+, as implemented in the HyperChem package. Two situations were considered: MD *in vacuo* and Langevin dynamics LD in water (friction coefficient 5.691 ps^{-1}), both with annealing or cooling time. The simulation temperature was 500K and the heating rate 0.1 to 500 K in 10 ps. Annealing rate was set 500 to 300K in 200 ps. Additional parameter settings are shown in Table 1; application of the lower values will be specified in due course.

Nile Red

PM3 calculations rendered conformations of NR such that the amino-group presented each ethyl pointing to opposite sides of the molecular plane in a twisted conformation. Instead, DFT optimizations often yielded both extreme methyls on the same side of the molecular plane and almost perpendicular to it, approaching a planar conformation. So, we kept account of both the twisting (θ) and the pyramidalization (δ) angles (Guido et al., 2010) of NR in the complexes (Figure 1). The θ angle is the dihedral C_A-C_A-N-C, and the δ angle is defined as the deviation from planarity of the three atoms bound to the amino-N atom, that is, (180° - |improper(C_A-N-C-C´|). Correspondingly, the dihedral θ´: C´$_A$-C_A-N-C´ for the other ethyl is defined.

RESULTS

Inclusion calculations

Semiempirical

The structures described are shown in Figures 2 to 7, left side: Figures 2 to 4 refer to NR:β-CD structures, Figures 5 to 7 shows NR:γ-CD structures.

The three complexes NR:β-CD # selected after the PM3 treatment presented the following features (later modified by DFT calculation): the amino group of NR showed a shallow insertion in the CD cavity. In structures 1 and 3 (for labels, Table 2, column 1), the guest appeared emerging through the secondary rim of the cycle; in structure 2, through the primary rim. In the latter structure the amino-N showed hydrogen (H) interaction with a primary OH group of β-CD.

The three complexes NR:γ-CD selected after the PM3 treatment presented the following features (later modified by DFT calculation): in structures 4 and 6, the guest entered deeply the γ-CD cavity -by the side of its amino

Table 1. Parameter settings for MD and LD.

Parameter (ps)	MD *in vacuo*	LD (water)
Run time	200 or 100	200
Time step	10^{-3}	10^{-3} or 10^{-4}

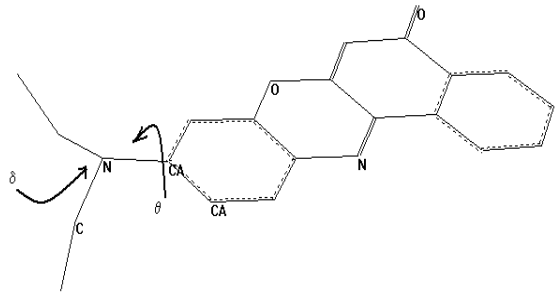

Figure 1. Nile Red and the twisting (θ) and pyramidalization (δ) angles.

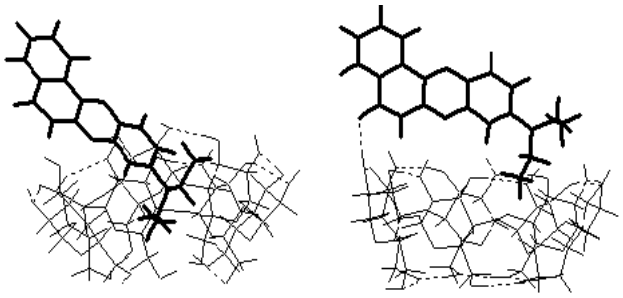

Figure 2. Complex NR:β-CD•1 according to PM3 (left) and DFT optimization (right); CD secondary rim up.

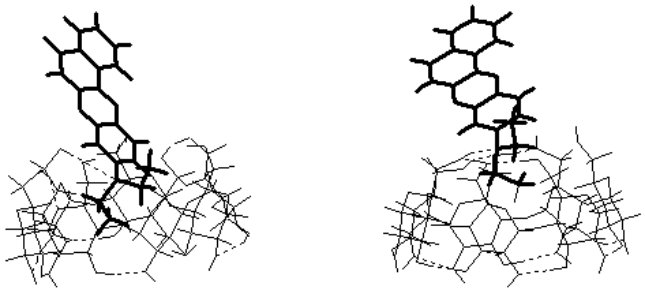

Figure 3. Complex NR:β-CD•2 according to PM3 (left) and DFT optimization (right); CD primary rim up.

group through the secondary rim (in 4) and the primary rim (in 6) of the cycle. Structure 6 showed H interaction between a primary OH group of γ-CD and the O-atom of the oxazinic heterocycle of NR. In complex 5, NR entered the cavity by the side of its condensed rings and showed deep insertion, too.

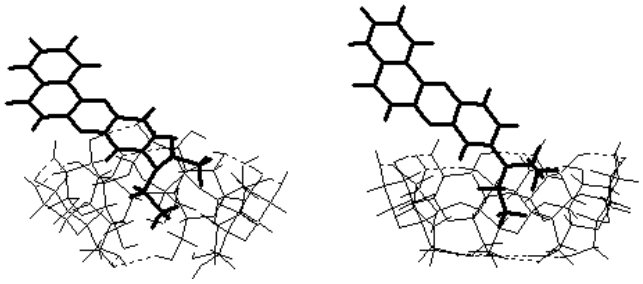

Figure 4. complex NR:β-CD•3 according to PM3 (left) and DFT optimization (right); CD secondary rim up.

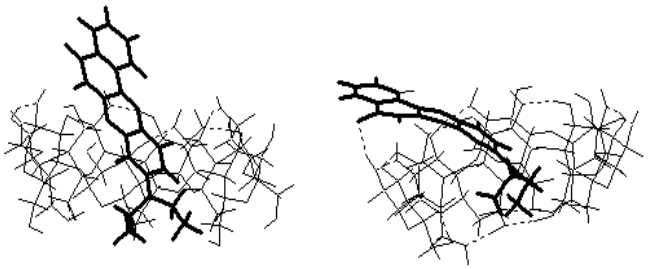

Figure 5. Complex NR:γ-CD•4 according to PM3 (left) and DFT optimization (right); CD secondary rim up.

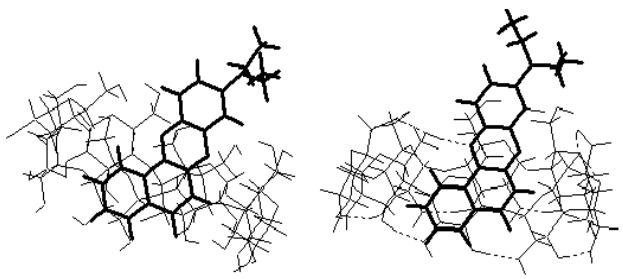

Figure 6. Complex NR:γ-CD 5 according to PM3 (left) and DFT optimization (right); CD primary rim up.

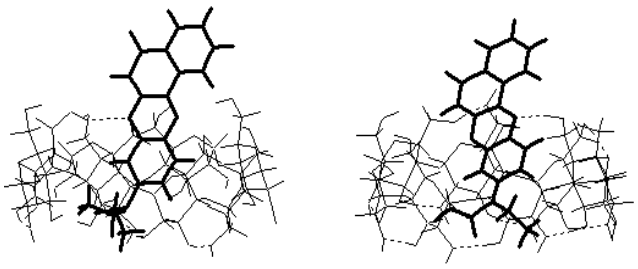

Figure 7. NR:γ-CD 6 complex according to PM3 (left) and DFT optimization (right); CD primary rim up.

The PM3 converged binding energies are shown in Table 2. The twisting θ and θ′ angles of NR, as well as the pyramidalization δ angle are shown in Table 3.

Table 2. Semiempirical PM3 binding energies and DFT energies (minima in *italics*) of inclusion complexes. Intermolecular H-bonds and interatomic distances.

NR in complex #	E(PM3) (kcal/mol)	Intermolecular H-bonding and X….H distance (Å)	E(DFT) (a.u.)	Intermolecular H-bonding and X….H distance (Å)
β-CD 1	-19072	-	-5306.60366283	C=O**….**HO 1.737
β-CD 2	-19069	Amino-N**….**HO 3.18	-5306.58017182	Amino-N**….**HO 1.849
β-CD 3	-19066	-	-5306.59130417	---
γ-CD 4	-21124	-	-5917.13957384	C=O**….**HO 1.983
γ-CD 5	-21122	-	-5917.14749763	Oxazine-N**….**HO 1.804
γ-CD 6	-21121	Oxazine-O**….**HO 2.64	-5917.13913407	Oxazine-N**….**HO 1.778

Table 3. Twisting (θ, θ') and pyramidalization (δ) angles (degrees) of the NR amino group in the inclusion complexes after PM3 (left column)/DFT (right column) calculations.

NR:CD complex #	θ:CA-CA-N-C		θ´:C´A-CA-N-C´		Improper angle CA-N-C-C´		δ	
β-CD 1	116.17	4.10	64.74	0.14	131	176	49	4
β-CD 2	36.94	27.72	85.45	71.20	-133	-136	47	44
β-CD 3	68.09	13.78	23.49	5.35	137	-172	43	8
γ-CD 4	116.21	3.17	149.85	12.09	-144	170	36	10
γ-CD 5	155.56	0.92	108.69	-4.17	133	-175	47	5
γ-CD 6	133.85	-10.02	89.05	-7.27	136	177	44	3

DFT

DFT treatment of the three complexes involving β-CD in Table 2, rendered NR:β-CD 1 the most stable, as shown in Table 2. However, the guest changed from a shallow inclusion to a rather occlusive location (Figure 2, right side). An intermolecular host-guest H-bond formed between carbonyl-O of NR and a secondary OH group of the cycle. The remote methyls of the amino group appeared both on the same side of the molecular plane of NR and the δ pyramidalization angle decreased notably (Table 3), towards a planar conformation. As for NR:β-CD 2, the guest kept the ethyl-groups oriented one above and the other below the molecular plane, the δ angle remained almost unchanged, and the amino-N tightened the H-bond with a primary OH group of the CD. This H-bond may explain the twisting and pyramidalization that the amino group preserved in this structure. After DFT treatment, complex NR:β-CD 3 changed mainly in the ethyls´ orientation; both last methyls appeared on the same side of the NR molecular plane, and the δ angle became much lower. The amino group could fit slightly twisted into the β-CD cavity.

Regarding NR:γ-CD complexes in Table 2, DFT optimization displaced NR:γ-CD 4 as the most stable conformer in this subset. The guest appeared less included, rather bent (Figure 5) and forming H-bond between the NR carbonyl-O and a secondary OH group of the cycle. Both amino-final-methyls of NR appeared on the same side of the molecular plane and the δ angle reveals a more sp^3-character of the amino-N. Structure 5 turned into the most stable one in this subset and an intermolecular H-bond between oxazine-N and a primary OH group was generated. The latter group appeared also involved in an intramolecular (intraCD) H-bond. This complex was the only one with the ring system of NR included in the cavity. The amino group approached a planar conformation. Finally, DFT optimization of

Table 4. Semiempirical PM3 binding energies and DFT energies (minima in *italics*) of NR:CD occlusion complexes. DFT intermolecular H-bonds and distances.

NR:CDocc complex #[a]	E(PM3) (kcal/mol)	E(DFT) (a.u.)	Intermolecular H-bonding[b]	O····H distance (Å)
β-CD o1/r2	-19065	-5306.60204537	C=O::::$(HO)_2$	1.663; 1.709
β-CD o2/r2	-19061	*-5306.62727285*	C=O::::$(HO)_2$	1.774; 1.791
β-CD o3/r1	-19058	-5306.57173199	-	-
β-CD o4/r1	-19055	-5306.59562289	C=O····HO	1.676
γ-CD o5/r2	-21119	*-5917.15033832*	C=O····HO	1.751
γ-CD o6/r1	-21116	-5917.13228360	-	-
γ-CD o7/r1	-21116	-5917.12238176	C=O····HO	1.708
γ-CD o8/r1	-21114	-5917.13089673	C=O::::$(HO)_2$	1.776; 1.807

[a] r1, r2 denote primary or secondary rim of CD. [b] C=O::::$(HO)_2$ denotes NR-carbonyl bound to two hydroxyl groups of CD.

Table 5. Twisting (θ, θ') and pyramidalization (δ) angles (degrees) of the amino group of NR in the occlusion complexes after PM3 (left column)/DFT (right column) calculations.

CD-NR occ complex #[a]	θ C_A-C_A-N-C		θ´ C´$_A$-C_A-N-C´		|improper angle|C_A-N-C-C´		δ	
β-CD o1/r2	-9.05	-2.14	-45.50	3.63	150	175	30	5
β-CD o2/r2	-27.44	4.95	-68.56	2.55	143	178	37	2
β-CD o3/r1	-101.0	1.24	-53.65	3.04	134	178	46	2
β-CD o4/r1	-46.91	7.25	-95.40	6.62	133	180	47	0
γ-CD o5/r2	-7.45	13.11	-44.01	-3.27	148	165	32	15
γ-CD o6/r1	27.06	-1.95	73.79	-4.05	136	179	44	1
γ-CD o7/r1	-6.01	-3.29	-44.47	-0.59	146	177	34	3
γ-CD o8/r1	42.87	5.66	5.15	1.45	147	176	33	4

[a] r1, r2 denote primary or secondary rim of CD.

Structure 6 changed the intermolecular H-bond between oxazine-O and a primary OH group of γ-CD, to oxazine-N and another primary OH group. As for the amino group, the δ angle was much decreased, and the terminal $–CH_3$ groups pointed at opposite directions one to the other, probably due to steric hindrance of the secondary rim to their rotation. The twist angles θ and θ', as well as δ appeared much lower.

Occlusion calculations

Table 4 (column 2) shows the energies yielded by our semiempirical calculations of the four more stable PM3 occlusion structures (labeled as occlusion #/rim #) involving NR with β-CD, and same number of structures involving NR with γ-CD. Each of the eight chosen complexes was later submitted to DFT optimization; the converged DFT energies and the H-bonds that were generated are also shown in Table 4. Table 5 shows the twisting θ and θ´, and the pyramidalization δ angles, according to PM3 and DFT optimizations of the eight complexes.

Figure 8 shows two DFT occlusion complexes of Table 4: β-CD o2/r2 and β-CD o1/r2, which are the most stable one (left structure) and the first less stable one (right structure). Similarly, Figure 9 shows NR:γ-CD occlusion complexes γ-CD o5/r2 and γ-CD o6/r1; r1 and r2 refer to interaction occurring either with primary or secondary rim. It thus becomes apparent that, regarding occlusion complexes and according to DFT results, interactions of NR with the secondary rim of both CDs tend to prevail. Additionally, interactions between NR and β-CD seem intensive, since double H-bonding between the C=O group and secondary hydroxyls occurred repeatedly. The most stable occlusion structure involving γ-CD showed one H-bond between NR and the host secondary rim. In this complex, the amino group least approached the planar conformation, probably due to interactions between the amino-N and one secondary hydroxyl (N····H distance: 2.172 Å), thus increasing the pyramidalization and twisting of the group.

Dynamics simulations

MD (*in vacuo*) and LD simulations of the three NR:γ-CD inclusion complexes shown in Table 2 led to the following results: complexes 4 and 5 converged, after the annealing, to the conformations shown in Figure 10 for

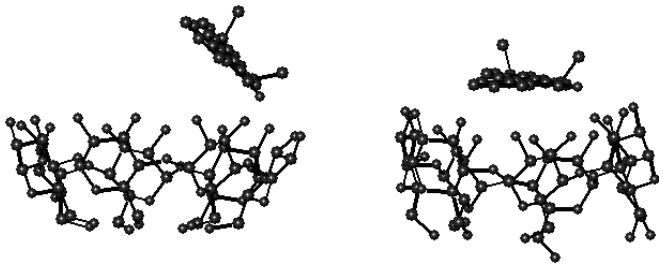

Figure 8. NR:β-CD o2/r2 (left) and NR:β-CD o1/r2 (right) occlusion complexes according to DFT optimization; H atoms are not shown (Table 4 for labeling).

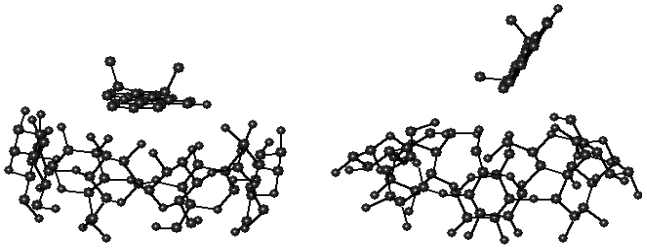

Figure 9. NR:γ-CD o5/r2 (left) and NR:γ-CD o6/r1 (right) occlusion complexes according to DFT optimization; H atoms are not shown.

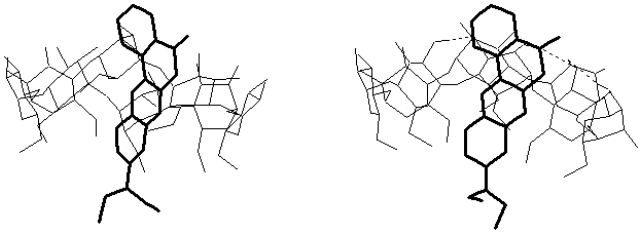

Figure 10. NR:g-CD 4 after MD (left) and LD (right); CD secondary rim up; H atoms not shown (Table 2 for labeling).

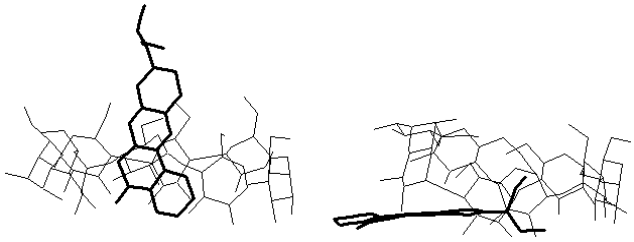

Figure 11. NR:γ-CD 5 after MD (left) and LD (right); primary rim up; H atoms not shown.

NR:γ-CD 4, and Figure 11 for NR:γ-CD 5. Figure 10 shows that both MD and LD yielded comparable inclusion structures. However, Figure 11 shows different results for MD and LD. The former preserved the inclusion complex

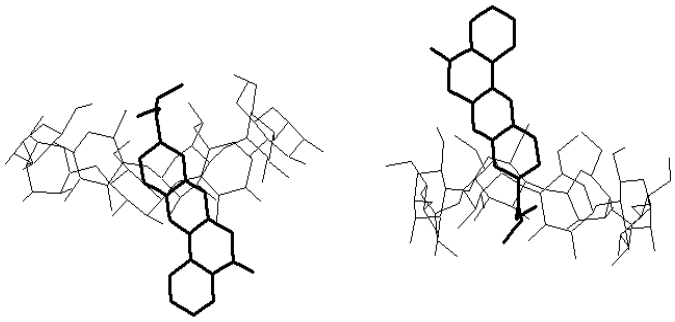

Figure 12. NR:γ-CD 6 after MD (left) and LD (right); primary rim up; H atoms not shown.

and the intermolecular oxazine-N····HO bond (N···H distance, 2.20Å); but LD (with time step 10^{-4} ps) rendered an occlusion complex with NR capping the secondary rim of CD.

As for dynamics treatment of NR:γ-CD 6, we firstly report about LD results (with time step 10^{-4} ps): the complex remained stable and the oxazine-O····HO bond was preserved (O···H distance, 2.22 Å). Referring to the MD simulation, at 160 ps run time, the complex dissociated definitely. So we performed another MD simulation with 100 ps run time. The inclusion complex remained stable, as shown in Figure 12. It is worth mentioning that during the latter simulation, the guest emerged out of the CD through the secondary rim –that is, the lower one in Figure 12 moved several times back and fro, rotated and finally re-entered the CD cavity by the side of the amino group remaining inside until the end of the run.

Table 6 shows the energies of these structures, after dynamics simulations.

DFT-B3LYP/6-31G calculation of NR

At the early stage of our analysis, we had optimized NR semiempirically (PM3) and used this structure for modeling the PM3 complexes. This NR conformer exhibited the amino group in twisted conformation; instead, DFT optimization of NR yielded a planar conformation of this group. Table 7 presents, for comparison, structural features of both conformers; values of PM3 (twisted) were obtained by DFT-B3LYP/6-31G energy calculation of the conformer as yielded by the earlier PM3 optimization.

DISCUSSION

Results suggest that inclusion complexes of NR and both CDs are possible, but occlusion complexes are more favourable, that is, energetically more stable for

Table 6. PM3 and DFT energies of NR:γ-CD inclusion complexes after MD and LD.

CD-NR complex #	EMD (kcal/mol)	EMD (a.u.)	ELD (kcal/mol)	ELD (a.u.)
γ-CD 4	-20733	-5916.20561612	-20689	-5916.11890542
γ-CD 5	-20740	-5916.31356455	-20718	-5916.26226222
γ-CD 6	-20727	-5916.19696961	-20690	-5916.16468285

Table 7. Structural parameters of twisted (*t*) and planar (*p*) NR conformers.

Conformer →	PM3(*t*)	DFT (*p*)	Literature values
Energy (au)	-1032.6234076	-1032.6458161	-
HOMO (au)	-0.20654	-0.19625	-
LUMO (au)	-0.09709	-0.09315	-
ΔE(LU-HO) (au)	0.10945	0.10310	0.1563(*t*), 0.1481(*p*)a/0.1007b
Dipole moment (D)	5.9800	9.2235	6.13(*t*), 8.23(*p*)a/8.7b
θ / θ' twist (deg)	-67.80 / -18.13	-1.50 / 1.71	5.8(average)b
δ pyramid.(deg)	47	2.4	0.3b

[a] Dias et al. (1999); [b]planar, as yielded by DFT-B3LYP hybrid functional calculation (Guido et al., 2010).

both CDs. H-bonding interactions of the carbonyl-oxygen of NR with the secondary hydroxyls of the CDs are apparent as well. In the case of β-CD occluded by NR, two concurrent H-bonds with two adjacent rim hydroxyls were obtained; instead, only one intermolecular H-bond was formed in the case of γ-CD. These features offer a chance to rationalize the different behaviour reported about the deactivation process of NR associated to β- or γ-CD after photon excitation during fluorescence experiments, as will be next discussed.

Formation of intermolecular H-bonding has been found to have a significant influence on the photophysical behaviour of various carbonyl compounds and has been reported to lead to efficient energy dissipation. Morimoito et al. (2001) analyzed molecules such as amino- or piperidino-anthraquinones, aminofluorenones and some other aromatic compounds with at least one carbonyl group in their structure, in presence of alcohols used as solvents. They found that the intermolecular H-bonding in the excited state is anisotropic with respect to the molecular plane. Detailed kinetic analyses of the fluorescence dynamic decay revealed that the intermolecular H-bonding involved two species with different lifetimes. They proposed two modes of interaction of Hydrogen with the carbonyl group: (1) an in-plane mode with the p_y orbital of the carbonyl-oxygen, and (2) an out-of-plane mode with the $\pi^*(p_z)$ molecular orbital. The former mode would give rise to an emissive species in the excited state (deactivation lifetime in the order of *ns*). The latter mode species (deactivation lifetime in the order of *ps*), would undergo an efficient deactivation process through the out-of-plane bending motion of the carbonyl group. Such H-bond would thus, perform as effective in coupling the excited state and the ground state to its high frequency and would enable the radiationless transition, that is, internal conversion.

Within this framework, we obtained that NR:β-CD most stable occlusion complexes have saturated the H-bonding capacity of the C=O group in the ground state, since NR appears anchored by two adjacent hydroxyls of the CD rim which have already established contact with the oxygen lone pairs. These complexes, after photoexcitation, could only deactivate via photoemission occurring on the *ns* timescale. Instead, NR:γ-CD most stable occlusion complexes show one carbonyl-oxygen lone pair implicated in H-bond. There is thus room for the out-of-plane interaction with some other close hydroxyl group of the CD rim, in the excited state. This would explain the difference between the radiative and non-radiative rate constants reported by Hazra et al. (2004), whose values suggest that radiative deactivation is relatively more favourable for NR:β-CD complexes, whereas non-radiative deactivation is more important, even enhanced (Srivatsavoy, 1999), in NR:γ-CD complexes.

Regarding the most stable inclusion complexes, probably less abundant, NR shows one intermolecular H-bond involving the carboxyl in the case of β-CD, and none involving the carboxyl in the case of γ-CD, before photoexcitation. In both such complexes, NR could undergo any of the two modes of interaction as described by Morimoito et al. (2001) with some close CD hydroxyl in the excited state, giving way to either radiative or non-radiative deactivation to the ground state.

Our DFT optimization of free NR yielded lower twisting angles and larger pyramidalization than reported by Guido et al. (2010). Intermolecular interactions in the complexes demand these angles to adapt accordingly;

this was especially evident in the occlusion NR:γ-CD most stable structure. If not engaged, the nitrogen atom in an intermolecular H-bond, the tendency of the amino group towards planar configuration is prevalent, no matter how many or where else other H-bonds involving NR may be present.

Conclusions

Regarding inclusion complexes, NR in β-CD is only partially inserted and by the side of the amino group. Intermolecular H-bonding between NR and the rim hydroxyls of the CDs occurs either via the carbonyl-oxygen or the amino-nitrogen of the guest. Inclusion complexes of NR with γ-CD can occur either by insertion of the guest´s amino group or, alternatively, of its condensed rings. H-bonding can form either with the carbonyl-oxygen or the oxazine-nitrogen. In these inclusion complexes, H-bonds appear simple.

Occlusion complexes are, however, more stable. Additionally, in these complexes the guest´s carbonyl-oxygen tends to form double H-bonds with β-CD, but simple H-bonds with γ-CD. Double H-bonds might be directly connected to NR radiative deactivation to the ground state after photoexcitation, whereas simple (or absent) H-bonds might include also the non-radiative deactivation process of NR. Which way NR deactivates, would depend on the feasible modes of interaction, in the excited state, between the carbonyl-oxygen of NR and the CD´s hydroxyls: only in-plane mode if the H-bond is double; either in- or out-of-plane, if the H-bond is simple.

Finally, the tendency of the amino group of NR towards planar configuration is prevalent, only modified when the nitrogen atom itself is involved in intermolecular H-bonding.

REFERENCES

Berger TA, Deye JF (1990). Composition and Density Effects using Methanol/Carbon Dioxide in Packed Column Supercritical Fluid Chromatography. Anal. Chem. 62:1181-1185.

Choi M, Jin D, Kim H, Kang TJ, Jeoung SC, Kim D (1997). Fluorescence Anisotropy of Nile Red and Oxazine 725 in an Isotropic Liquid Crystal. J. Phys. Chem. B 101:8092-8097.

Cser A, Nagy K, Biczók L (2002). Fluorescence lifetime of Nile Red as a probe for the hydrogen bonding strength with its microenvironment. Chem. Phys. Lett. 360:473-478.

Datta A, Mandal D, Pal SK, Bhattacharyya K (1997). Intramolecular Charge Transfer Processes in Confined Systems. Nile Red in Reverse Micelles. J. Phys. Chem. B 101:10221-10225.

Deye JF, Berger TA, Anderson AG (1990). Nile Red as solvatochromic dye for measuring solvent strength in normal liquids and mixtures of normal liquids with supercritical fluids and near critical fluids. Anal. Chem. 62:615-622.

Dias Jr. LC, Custodio R, Pessine FBT (1999). Theoretical studies of Nile Red by *ab initio* and semiempirical methods. Chem. Phys. Lett. 302:505-510.

Dias Jr. LC, Custodio R, Pessine FBT (2006). Investigation of the Nile Red Spectra by Semi-empirical Calculations and Spectrophotometric Measurements. Int. J. Quant. Chem. 106:2624-2632.

Duchêne D Ed. (1987). Cyclodextrin and their Industrial Uses; Editions de Santé:Paris. pp. 297-350.

Dutta AK, Kamada K, Ohta K (1996). Spectroscopic studies of nile red in organic solvents and polymers. J. Photochem. Photobiol. A: Chem. 93:57-64.

Freeman DM, Kroe RR, Ruffles R, Robson J, Coleman JR, Grygon CA (2001). A fluorescence method for probing the effect of small molecules on DPPC lipid bilayers using the hydrophobic dye, Nile Red. Biophys. J. 80:2375-Pos, p. 527a; last accessed January 2012 at:http://www.ncbi.nlm.nih.gov/pmc/articles/PMC1914015/pdf/biophysj00804-0558.pdf.

Gaussian 03, Revision A.1. Frisch MJ, Trucks GW, Schlegel HB, Scuseria GE, Robb MA, Cheeseman JR, Montgomery Jr. JA, Vreven T, Kudin KN, Burant JC, Millam JM, Iyengar SS, Tomasi J, Barone V, Mennucci B, Cossi M, Scalmani G, Rega N, Petersson GA, Nakatsuji H, Hada M, Ehara M, Toyota K, Fukuda R, Hasegawa J, Ishida M, Nakajima T, Honda Y, Kitao O, Nakai H, Klene M, Li X, Knox JE, Hratchian HP, Cross JB, Adamo C, Jaramillo J, Gomperts R, Stratmann RE, Yazyev O, Austin AJ, Cammi R, Pomelli C, Ochterski JW, Ayala PY, Morokuma K, Voth GA, Salvador P, Dannenberg JJ, Zakrzewski VG, Dapprich S, Daniels AD, Strain MC, Farkas O, Malick DK, Rabuck AD, Raghavachari K, Foresman JB, Ortiz JV, Cui Q, Baboul AG, Clifford S, Cioslowski J, Stefanov BB, Liu G, Liashenko A, Piskorz P, Komaromi I, Martin RL, Fox DJ, Keith T, Al-Laham MA, Peng CY, Nanayakkara A, Challacombe M, Gill PMW, Johnson B, Chen W, Wong MW, Gonzalez C, Pople JÁ (2003). Gaussian Inc, Pittsburgh PA.

Greenspan P, Fowler SD (1985). Spectrofluorometric studies of the lipid probe, nile red. J. Lipid Res. 26:781-789.

Guido CA, Mennucci B, Jacquemin D, Adamo C (2010). Planar *vs*. twisted intramolecular charge transfer mechanism in Nile Red:new hints from theory. Phys. Chem. Chem. Phys. 12:8016-8023.

Harata K (1991). Recent Advances in the X-ray analysis of cyclodextrin complexes. In Inclusion Compounds; Atwood JL, Davies JED, MacNicol DD, Eds.; Academic Press: London. 5:311-344.

Hazra P, Chakrabarty D, Chakraborty A, Sarkar N (2004). Intramolecular charge transfer and solvation dynamics of Nile Red in the nanocavity of cyclodextrins. Chem. Phys. Lett. 388:150-157.

HyperChem 6 Pro, Hypercube, Inc., Serial # 12-600-1500700081.

Johnson SR, Sutter JM, Engelhardt HL, Jurs PC, White J, Kauer JS, Dickinson TA, Walt DR (1997). Identification of Multiple Analytes Using an Optical Sensor Array and Pattern Recognition Neural Networks. Anal. Chem. 69:4641-4648.

Kawski A, Bojarski P, Kukliński B (2008). Estimation of ground- and excited-state dipole moments of Nile Red dye from solvatochromic effect on absorption and fluorescence spectra. Chem. Phys. Lett. 463:410-412.

Kawski A, Kukliński B, Bojarski P (2009). Photophysical properties and thermochromic shifts of electronic spectra of Nile Red in selected solvents. Excited states dipole moments. Chem. Phys. 359:58-64.

Kipkemboi PK, Easteal AJ (1994). Solvent Polarity Studies of the Water+t-Butyl Alcohol and Water+t-Butylamine Binary Systems with the Solvatochromic Dyes Nile Red and Pyridinium-N-phenoxide Betaine Refractometry and Permittivity Measurements. Aust. J. Chem. 47:1771-1781.

Korth M (2010). Third-Generation Hydrogen-Bonding Corrections for Semiempirical QM Methods and Force Fields. J. Chem. Theory Comput. 6:3808-3816.

Li XS, Mu TW, Guo QX (2000). A systematic quantum chemistry study on cyclodextrins. Monats. Chem. 131:849-855.

Maiti NC, Krishna MMG, Britto PJ, Periasamy N (1997). Fluorescence Dynamics of Dye Probes in Micelles. J. Phys. Chem. B 101:11051-11060.

Matsui K, Nozawa K (1997). Molecular Probing for the Microenvironment of Photonics Materials Prepared by the Sol-Gel Process. Bull. Chem. Soc. Jpn. 70:2331-2335.

McNamara JP, Hillier IH (2007). Semi-empirical molecular orbital methods including dispersion corrections for the accurate prediction of the full range of intermolecular interactions in biomolecules. Phys. Chem. Chem. Phys. 9:2362-2370.

Meinershagen JL, Bein T (1999). Optical Sensing in Nanopores. Encapsulation of the Solvatochromic Dye Nile Red in Zeolites. J. Am.

Chem. Soc. 121:448-449.
Morimoito A, Yatsuhashi T, Shimada T, Biczók L, Tryk D, Inoue H (2001). Radiationless Deactivation of an Intramolecular Charge Transfer Excited State through Hydrogen Bonding: Effect of Molecular Structure and Hard-Soft Anionic Character in the Excited State. J. Phys. Chem. A. 105:10488-10496 (and references therein).
Morley JO, Morley RM, Docherty R, Charlton MH (1997). Fundamental Studies on Brooker's Merocyanine. J. Am. Chem. Soc. 119:10192-10202.
Morpurgo S, Bossa M, Morpurgo GO (1998). Critical test of PM3-calculated proton transfer activation energies: A comparison with ab initio and AM1 calculations. J. Molec. Struct. (THEOCHEM) 429:71-80.
Saenger W (1980). Cyclodextrins in research and industry. Angew. Chem. Int. Ed. Engl. 19:344-362.
Saenger W (1984). Structural aspects of cyclodextrins and their inclusion complexes. Inclusion Compounds; Atwood JL, Davies JED, MacNicol DD, Eds.; Academic Press: London. 2:231-260.
Saenger W, Jacob J Gessler K, Steiner T, Hoffmann D, Sanbe H, Koizumi K, Smith SM Takaha T (1998). Structures of the Common Cyclodextrins and Their Larger Analogues - Beyond the Doughnut. Chem. Rev. 98:1787-1802.
Srivatsavoy VJP (1999). Enhancement of excited state nonradiative deactivation of Nile Red in γ-cyclodextrin:evidence for multiple inclusion complexes. J. Lumin. 82:17-23.
Szejtli J (1988). Cyclodextrin Technology; Kluwer Academic Publishers: Dordrecht.
Szejtli J (1998). Introduction and General Overview of Cyclodextrin Chemistry. Chem. Rev. 98:1743-1753.
Uppili S, Thomas KJ, Crompton EM, Ramamurthy V (2000). Probing Zeolites with Organic Molecules:Supercages of X and Y Zeolites Are Superpolar. Langmuir 16:265-274.
Uusi-Penttilä MS, Richards RJ, Torgerson BK, Berglund KA (1997). Spectroscopically Determined Dielectric Constants for Various Esters. Ind. Eng. Chem. Res. 36:510-512.
Wagner BD, Stojanovic N, LeClair G, Jankowski CK (2003). A Spectroscopic and Molecular Modelling Study of the Nature of the Association Complexes of Nile Red with Cyclodextrins. J. Incl. Phenom. Macrocycl. Chem. 45:275-283.
White J, Kauer JS, Dickinson TA, Walt DR (1996). Rapid Analyte Recognition in a Device Based on Optical Sensors and the Olfactory System. Anal. Chem. 68:2191-2202.
Yanai T, Tew DP, Handy NC (2004). A new hybrid exchange-correlation functional using the Coulomb-attenuating method (CAM-B3LYP). Chem. Phys. Lett. 393:51-57.
Zheng YJ, Merz Jr. KM (1992). Study of hydrogen bonding interactions relevant to biomolecular structure and function. J. Comp. Chem. 13:1151-1169.